J|A|C|S
ARTICLES

Published on Web 05/19/2010

# Conformations of End-Tethered DNA Molecules on Gold Surfaces: Influences of Applied Electric Potential, Electrolyte Screening, and Temperature

Wolfgang Kaiser and Ulrich Rant*

*Walter Schottky Institut, Technische Universität München, Am Coulombwall 3, 85748 Garching, Germany*

Received October 13, 2009; E-mail: rant@wsi.tum.de

***Abstract:*** We describe the behavior of 72mer oligonucleotides that are end-tethered to gold surfaces under the influence of applied electric fields. The DNA extension is measured by fluorescence energy transfer as a function of the DNA hybridization state (single- and double-stranded), the concentration of monovalent salt in solution (100 $\mu$M to 1 M NaCl), the applied electrode potential (−0.6 to +0.1 V vs Pt), and the temperature (1 to 50 °C). At high ionic strength, the DNA conformations are very robust and independent of the applied electrode potential and temperature variations. In solutions of medium ionic strength, the DNA conformation can be manipulated efficiently by applying bias potentials to the Au electrodes. The molecules are repelled at negative potentials and attracted to the surface at positive potentials. The conformation transition occurs abruptly when the electrode bias is swept by merely 0.1 V across the transition potential, which shifts negatively when the salinity is decreased. The behavior can be understood by electrostatic screening arguments and, in the case of single-stranded DNA, when secondary structures are taken into account. At low ionic strength, the experiments reveal an intriguing temperature-dependent stiffening of single-stranded DNA, which can be rationalized by combining counterion condensation theory with the Odjik−Skolnick−Fixman description of the electrostatic persistence length and the unstacking of bases at elevated temperatures.

## Introduction

DNA monolayers anchored on solid supports are a paradigm of functional molecular interfaces with multifaceted physical and chemical properties. Although they have already found their way into important applications like DNA microarray technology, their full potential has not been tapped yet. Owing to their charged nature, surface-tethered DNA layers can be manipulated efficiently through the application of electric fields—a possibility that is under-explored up to now—and by this means can be turned from passive layers into actively controlled nano−bio interfaces with improved functionality. A decade ago, it was observed that DNA layers respond to externally applied electrical potentials[1] and that electric potential control can be used to manipulate and probe the binding efficiency/specificity of complementary DNA strands[2,3] or facilitate transport of target DNAs to sensor surfaces.[4] Since then, the consequences of applied electric fields on the DNA conformation have been recognized in a number of studies involving scanning probe microscopy,[5,6] fluorescence,[7−10] or surface plasmon resonance techniques.[3,11] DNA layers have been reported to exhibit persistent electrical conformation switching,[8,12] with applications in DNA and protein sensing.[13,14] Electrically induced conformation changes of DNA molecules on metal surfaces have also been found to be of importance to electrochemical biosensing assays and should accounted for in the design of novel sensing concepts.[15,16] Despite many promising results and growing interest, we are still lacking a detailed understanding about the parameters that govern the behavior of DNA on electrically biased surfaces.

(1) Kelley, S. O.; Barton, J. K.; Jackson, N. M.; McPherson, L. D.; Potter, A. B.; Spain, E. M.; Allen, M. J.; Hill, M. G. *Langmuir* **1998**, *14*, 6781–6784.
(2) Sosnowski, R. G.; Tu, E.; Butler, W. F.; Oconnell, J. P.; Heller, M. J. *Proc. Natl. Acad. Sci. U.S.A.* **1997**, *94*, 1119–1123.
(3) Heaton, R. J.; Peterson, A. W.; Georgiadis, R. M. *Proc. Natl. Acad. Sci. U.S.A.* **2001**, *98*, 3701–3704.
(4) Edman, C. F.; Raymond, D. E.; Wu, D. J.; Tu, E. G.; Sosnowski, R. G.; Butler, W. F.; Nerenberg, M.; Heller, M. J. *Nucleic Acids Res.* **1997**, *25*, 4907–4914.
(5) Wackerbarth, H.; Grubb, M.; Zhang, J. D.; Hansen, A. G.; Ulstrup, J. *Langmuir* **2004**, *20*, 1647–1655.
(6) Zhang, Z. L.; Pang, D. W.; Zhang, R. Y.; Yan, J. W.; Mao, B. W.; Qi, Y. P. *Bioconjugate Chem.* **2002**, *13*, 104–109.
(7) Moiseev, L.; Unlu, M. S.; Swan, A. K.; Goldberg, B. B.; Cantor, C. R. *Proc. Natl. Acad. Sci. U.S.A.* **2006**, *103*, 2623–2628.
(8) Murphy, J. N.; Cheng, A. K. H.; Yu, H. Z.; Bizzotto, D. *J. Am. Chem. Soc.* **2009**, *131*, 4042–4050.
(9) Rant, U.; Arinaga, K.; Fujita, S.; Yokoyama, N.; Abstreiter, G.; Tornow, M. *Org. Biomol. Chem.* **2006**, *4*, 3448–3455.
(10) Wang, K.; Goyer, C.; Anne, A.; Demaille, C. *J. Phys. Chem. B* **2007**, *111*, 6051–6058.
(11) Yang, X. H.; Wang, Q.; Wang, K. M.; Tan, W. H.; Yao, J.; Li, H. M. *Langmuir* **2006**, *22*, 5654–5659.
(12) Rant, U.; Arinaga, K.; Fujita, S.; Yokoyama, N.; Abstreiter, G.; Tornow, M. *Nano Lett.* **2004**, *4*, 2441–2445.
(13) Rant, U.; Arinaga, K.; Scherer, S.; Pringsheim, E.; Fujita, S.; Yokoyama, N.; Tornow, M.; Abstreiter, G. *Proc. Natl. Acad. Sci. U.S.A.* **2007**, *104*, 17364–17369.
(14) Rant, U.; Pringsheim, E.; Kaiser, W.; Arinaga, K.; Knezevic, J.; Tornow, M.; Fujita, S.; Yokoyama, N.; Abstreiter, G. *Nano Lett.* **2009**, *9*, 1290–1295.
(15) Cash, K. J.; Ricci, F.; Plaxco, K. W. *J. Am. Chem. Soc.* **2009**, *131*, 6955–6957.
(16) Drummond, T. G.; Hill, M. G.; Barton, J. K. *Nat. Biotechnol.* **2003**, *21*, 1192–1199.

  

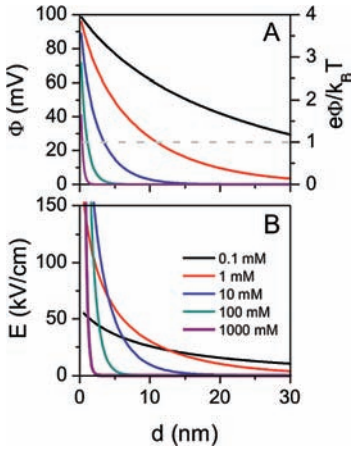


***Figure 1.*** Gouy−Chapman potential Φ (A) and electric field $E$ (B) in electrolyte solution plotted as a function of the distance $d$ to a surface which is biased at 100 mV. Curves are calculated for solutions containing varying concentrations of monovalent salt. The right scale in panel A shows the electrostatic energy of one elementary charge normalized by the thermal energy $k_BT$ at room temperature.

Although it is plausible that a charged molecule tethered to a charged surface must experience electric forces of some kind, it is interesting to note how extreme the conditions at an electrically polarized metal/solution interface in fact are. Electrical interactions between charged objects in salt solutions are governed by screening effects; that is, free ions in solution redistribute around charged objects and form screening layers. At flat polarized interfaces, the diffusive potential distribution Φ on the solution side is described by the Gouy−Chapman equation,

$$\Phi(d) = \frac{2kT}{e}\ln\left(\frac{1+\gamma\exp(-d/l_D)}{1-\gamma\exp(-d/l_D)}\right), \quad \gamma = \tanh\left(\frac{e\Phi_0}{4k_BT}\right) \tag{1}$$

where the Debye length $l_D$ is a characteristic screening length that depends on the salt concentration (ionic strength),

$$l_D^2 = \frac{\varepsilon\varepsilon_0 k_B T}{2ne^2} \qquad \text{for a monovalent (1,1) salt} \tag{2}$$

where $d$ denotes the distance to the surface, $\Phi_0$ is the surface potential, and $n$ is the ion density.

Figure 1 depicts the Gouy−Chapman result for varying concentrations of monovalent salt assuming a surface potential $\Phi_0 = 100$ mV. The potential (panel A) is strongly localized within the first few nanometers from the surface and drops quickly on the length scale of oligonucleotides. Comparing the electric energy of an elementary charge to $k_BT$ (right scale, Figure 1A) underlines the short-ranged character of electric interactions. A few nanometers from the surface, Brownian motions prevail over electric forces and dominate the system behavior. At the same time, the rapid decay of the potential generates remarkably high electric fields—and strong field gradients—which can exceed 100 kV/cm (Figure 1B). Consequently, the DNA resides in a highly non-uniform electrostatic environment where the surface proximal part is exposed to significantly stronger electric forces than distal DNA segments. From a polymer physics point of view, DNA represents an interesting model system for a highly charged linear macromolecule (polyelectrolyte). Its intrinsic electrostatic self-energy is so high that counterion condensation phenomena come into play which reduce the effective charge density.[17] The distinct rigidity of single-stranded DNA (ss-DNA) and double-stranded DNA (ds-DNA) means that, on the length scale of oligonucleotides, DNA appears in two different mechanical conformations; i.e., ss-oligonucleotides are flexible, while ds-oligonucleotides are stiff and rod-like. In conjunction, this sets the stage for an intriguing behavior of DNA at electrically polarized interfaces.

Here we systematically study the influence of externally applied surface potential and the consequences of varying solution salinity as well as temperature on the conformation of DNA layers comprising 72mer nucleotides. Special care has been taken to prepare ultra-low-density DNA layers so that interactions between DNA molecules on the surface (crowding) can be excluded. The experimental results and discussion are arranged according to the content of monovalent salt (NaCl) in the electrolyte solution and follow electrostatic screening arguments.

## Materials and Methods

**DNA Sequence and Melting.** Single-stranded DNA, labeled with a Cy3 fluorescence dye and a thiol linker at opposite ends, was obtained from IBA GmbH (Göttingen, Germany). The sequence of the 72mer oligonucleotide was selected with the intention to minimize the occurrence of complicating secondary structures: 5′-HS-$(CH_2)_6$-TAG TCG TGA GCA CAT GGA CCT GAT TAG TCG TAA GCT GAT ATG GCT GAT TAG TCG GAA GCA TCG-Cy3-3′. A sequence analysis using the DINAmelt software package[18,19] (http://dinamelt.bioinfo.rpi.edu/) identified several thermally stable structures with predicted melting temperatures ranging from 20 to 64 °C, depending on the solution's salinity. The most stable secondary structures and corresponding thermodynamic data are displayed in the Supporting Information, Figure S1 and Table S1. Additionally, possible secondary structures (hairpins and self-annealing sites) of the ss-DNA were examined experimentally by conducting thermal denaturation (melting temperature) measurements in solution. A UV−vis absorption spectrometer (Varian Cary 50) equipped with a temperature-controlled holder for 1 cm cuvettes was used to monitor the hypochromic effect at 260 nm. Temperatures were increased from 1 to 80 °C at a rate of 0.5 °C/min under continuous stirring. The concentrations of DNA and added salt were [DNA] = 250 nM and [NaCl] = 0.1, 1, 10, 100, and 1000 mM. The stability of ds-DNA was determined in an analogous manner. ds-DNA was prepared by hybridizing ss-DNA with its complementary sequence (cs-DNA): [ss-DNA] = [cs-DNA] = 125 nM. Hybridization reactions in 100 mM and 1 M NaCl solutions were facilitated by heating the solutions to 70 °C, i.e., above the melting temperature of the most stable secondary structures in the ss-DNA ($T_m$ = 49 °C in 1 M NaCl). After 30 min the samples were slowly cooled to room temperature within 1.5 h. For the experiments at final NaCl concentrations of 10 mM, the DNA was hybridized in [NaCl] = 100 mM solution and subsequently diluted to [NaCl] = 10 mM before melting experiments. Characteristic signatures of duplex melting were not found at lower concentrations of NaCl, indicating that the ds-DNA helix is not stable under these conditions.

**Preparation of Low-Density DNA Layers.** Gold working electrodes of 500 $\mu$m diameter were fabricated on single-crystalline sapphire wafers by subsequently depositing thin films of titanium (10 nm) and gold (300 nm) with standard optical lithography and metallization techniques. Before the adsorption of DNA onto the gold electrodes, the wafer was consecutively cleaned with piranha

(17) Manning, G. S. *Q. Rev. Biophys.* **1978**, *11*, 179–246.
(18) Markham, N. R.; Zuker, M. *Nucleic Acids Res.* **2005**, *33*, W577–W581.
(19) Markham, N. R.; Zuker, M. In *Bioinformatics, Vol. 2. Structure, Function and Applications*; Keith, J. M., Ed.; Humana: Totowa, NJ, 2008; pp 3−31.

solution ($H_2SO_4$ [95%]:$H_2O_2$ [30%] = 2:1) and $HNO_3$ (60%) for 15 min, followed by thorough rinsing with deionized water.

Double-stranded DNA was prepared by hybridizing ss-DNA (20 $\mu$M) with an excess amount of cs-DNA (27 $\mu$M) in buffer solution (200 mM NaCl, 10 mM Tris, pH = 7.3). The solution was heated to 60 °C (5 min) and slowly annealed to room temperature (5 h). Self-assembled DNA layers were formed by exposing the gold electrodes to Tris-buffered solution ([Tris] = 10 mM, [NaCl] = 200 mM, pH = 7.3) containing 1 $\mu$M ds-DNA. In a second step, mercaptohexanol (MCH) was co-adsorbed onto the DNA-modified gold electrodes by exposing the electrodes to a Tris buffer solution (10 mM Tris, 50 mM NaCl, pH = 7.3) containing 1 mM MCH for 1 h. The formation of a dense MCH sublayer passivates the gold electrodes and prevents nonspecific interactions between DNA and the gold surface.[20] In a final step, we electrically desorbed a part of the densely packed DNA layer to produce low-density DNA layers. To this end, negative potentials (−0.9 to −1.1 V vs Pt) were repeatedly applied to the Au working electrodes in a solution containing 1 mM MCH. This triggered the release of DNA from the surface and covered the vacant sites with MCH.[21] After an electrical desorption step had been performed, the resulting DNA density was probed by "switching" experiments.[12] Here, alternating negative and positive potentials were applied to the electrodes, and concurrent changes in the DNA layer conformation were determined by monitoring the attainable fluorescence modulation, $\Delta F$. It is known from previous investigations that the relative modulation amplitude $\Delta F/F$ saturates at a maximum when the packing density is reduced to a critical value below which steric interactions between individual DNA molecules on the surface do not occur anymore.[12,22] Thus, desorption and switching cycles were repeated until a maximal $\Delta F/F$ value was observed. In this state, the DNA molecules do not interact sterically with neighboring strands, and crowding effects are avoided. Fluorescence imaging of DNA layers prepared by this procedure revealed intensity variations of <20% (120 $\mu$m spot), suggesting that the DNA's density heterogeneity is <20% (see Figure S5 in the Supporting Information). From previous measurements,[21] we can estimate an upper limit for the surface density of $10^{11}$ molecules/cm$^2$, which corresponds to an average inter-strand distance of more than 30 nm. Consequently, although an ensemble of roughly $10^8$ DNA strands is probed simultaneously on electrodes of 500 $\mu$m diameter, the molecules are expected to behave as individual entities.

Measurements were first carried out with ds-DNA layers. Afterward, the DNA was denatured (dehybridized) by elevating the temperature to 50 °C and rinsing the surface extensively with 0.1 mM NaCl solution, which produced ss-DNA layers.

**Electrochemical Cell.** Electrical potentials were applied with a commercially available potentiostat (PGSTAT30, Autolab, The Netherlands) to a gold electrode (0.2 mm$^2$) vs a MCH-coated platinum quasi-reference electrode (2.2 mm$^2$) which surrounded the working electrode (two-electrode configuration). The offset of the MCH-coated Pt quasi-reference with respect to a saturated Ag/AgCl electrode was checked (in a three-electrode configuration) in solutions of varying salinity and found to be constant at 0.42 ± 0.04 V up to 10 mM NaCl and then drop slightly to 0.40 ± 0.04 and 0.36 ± 0.04 V for 100 and 1000 mM NaCl, respectively. This trend can be attributed to the adsorption of $Cl^-$ onto the Pt surface;[23] however, due to passivation of the surface by the MCH layer which also covers the Pt electrodes, the effect is comparably small and is neglected in the following. The MCH-passivated electrodes exhibited characteristics of ideally polarizable electrodes in the examined voltage regime; i.e., Faradaic currents were not detectable in 50 mM NaCl solution within the sensitivity range (below 1 nA) of the potentiostat used.

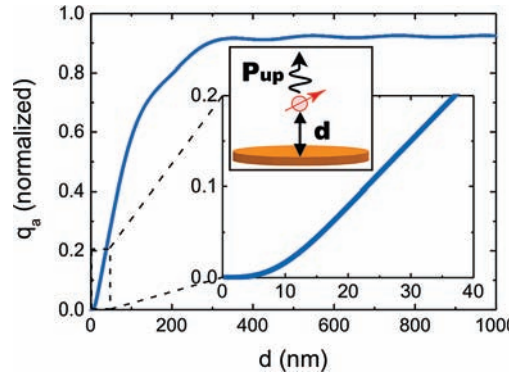


***Figure 2.*** Calculated apparent quantum yield $q_a$ of an isotropically oriented dipole (red), located at distance $d$ above a gold surface. $P_{up}$ denotes the power radiated into the upper half space.

**Layer Height Analysis by Fluorescence Energy Transfer.** The molecular extension from the surface is measured in a contactless mode by observing the fluorescence of dyes attached to the grafted DNA's distal ends. The fluorescence strongly depends on the distance between the dye and the gold surface due to non-radiative energy transfer from the dye to the gold (coupling to surface plasmons). The distance dependence of the radiative decay can be calculated by treating the dye as an oscillating, damped electric dipole above the gold surface.[24−27] When the dipole approaches the metal surface closer than approximately one wavelength of the emitted light, evanescent components of the dipole field interact with the gold layer, and energy from the dipole can be absorbed by the gold film or transformed into plasmon excitations propagating at the film surface. The power radiated by the dipole into the upper half-sphere from the surface, $P_{up}$, is the experimentally observable quantity. It is related to the apparent quantum yield, $q_a$, and totally radiated power, $P$, by $q_a = P_{up}/P$. We calculated the distance dependence of $q_a$ employing expressions given by Novotny[26,27] using the following parameters: emission wavelength of Cy3, $\lambda$ = 565 nm; dielectric constants of gold, $\varepsilon_{Au} = -6.7 + i1.9$[28,29] and water, $\varepsilon_{H_2O} = 1.8$ at $\lambda$ = 565 nm. We assumed an isotropic dipole orientation since the dye is attached to the DNA's distal end by a flexible linker, which allows for an almost free rotation of the dye. Figure 2 shows the calculated apparent quantum yield that was used to convert the measured fluorescence intensity to the distance of the dye to the gold surface, i.e., layer height (see Figure S2 in the Supporting Information for parallel and perpendicular dipole orientations). The quenching region, where energy transfer due to near-field coupling occurs, extends to roughly 100 nm from the surface; for larger distances, damped interference oscillations are seen. Even in the far-field the quantum yield does not reach 100% because of absorption by the lossy Au film, which is a non-ideal mirror. For practical reasons, we used the simple analytical function $q_a(d) = 0.45(1 - \exp(-0.042d))^{3.1}$ ($d$ in nm) to approximate the numerically calculated results in the distance range of interest ($d$ < 40 nm), which deviates from the calculated values by less than 10% (see Figure S2 in the Supporting Information). Before performing the fluorescence-to-height conversion, the background was subtracted and the measured fluorescence was corrected for

(20) Herne, T. M.; Tarlov, M. J. *J. Am. Chem. Soc.* **1997**, *119*, 8916–8920.
(21) Arinaga, K.; Rant, U.; Knezevic, J.; Pringsheim, E.; Tornow, M.; Fujita, S.; Abstreiter, G.; Yokoyama, N. *Biosens. Bioelectron.* **2007**, *23*, 326–331.
(22) Rant, U.; Arinaga, K.; Fujita, S.; Yokoyama, N.; Abstreiter, G.; Tornow, M. *Langmuir* **2004**, *20*, 10086–10092.
(23) Shi, Z. C.; Lipkowski, J. *J. Electroanal. Chem.* **1996**, *403*, 225–239.
(24) Chance, R. R.; Prock, A.; Silbey, R. In *Advances in Chemical Physics*; Prigogine, I., Rice, S. A., Eds.; Wiley: New York, 2007; pp 1−65.
(25) Sullivan, K. G.; Hall, D. G. *J. Opt. Soc. Am. B* **1997**, *14*, 1149–1159.
(26) Novotny, L. *J. Opt. Soc. Am. A−Opt. Image Sci. Vision* **1997**, *14*, 91–104.
(27) Novotny, L. *Principles of Nano-Optics*; Cambridge University Press: Cambridge, UK, 2006.
(28) Etchegoin, P. G.; Le Ru, E. C.; Meyer, M. *J. Chem. Phys.* **2006**, *125*.
(29) Johnson, P. B.; Christy, R. W. *Phys. Rev. B* **1972**, *6*, 4370–4379.

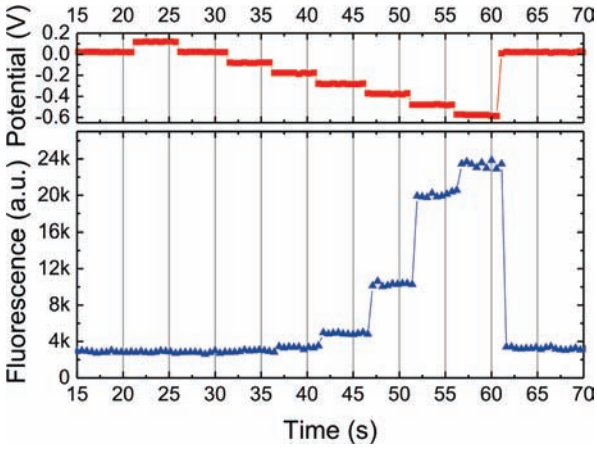


***Figure 3.*** Lower panel: Fluorescence emission from a dye-labeled 72 base-pair ds-DNA layer tethered to a gold surface. Upper panel: Potentials applied to the DNA/MCH-coated gold electrode vs a MCH-coated Pt quasi-reference electrode (Pt $\approx +0.4$ V vs Ag/AgCl). [NaCl] = 10 mM, $T = 20$ °C.

several factors that influence the emission of the DNA-coupled Cy3 dye. These corrections are described in detail in the Supporting Information and take into account the temperature dependence of Cy3 fluorescence (Figure S3), the salinity of the electrolyte solution (Figure S1), and the hybridization state of the DNA (Figures S3 and S4). Briefly, salinity variations do not affect the Cy3 fluorescence significantly; the hybridization of Cy3-labeled ss-DNA with unlabeled complement causes the Cy3 fluorescence to drop by ca. 30%; elevating the temperature from 1 to 50 °C causes the Cy3 fluorescence to drop by roughly 70%. Photobleaching effects were checked before and after measurements and found to be negligible.

The described procedures allow for a relative comparison of layer heights but do not provide absolute height values. In order to calibrate the height measurements, we used the fluorescence intensity measured for the 72 base pair (bp) ds-DNA layer at negative electrode potentials and low-salinity conditions (10 mM NaCl). Under these conditions, it is plausible that the DNA stands upright on the surface, as will become evident from the discussion below; thus, the layer height roughly corresponds to the molecular contour length of the 72 bp duplex, i.e., 24 nm. We note that the accuracy of the employed method to infer the layer height from fluorescence intensity may be limited and that all reported height values may be flawed by a systematic error of a few tens percent; however, such an error would not affect the conclusions of this work.

## Results

Figure 3 shows a representative measurement conducted to probe the influence of electric fields on the conformation of DNA molecules on a gold surface. The fluorescence emitted from a double-stranded 72 bp DNA layer is measured while a staircase-like sequence of bias potentials is applied to the supporting gold electrode. At positive potentials the fluorescence intensity is low, which indicates that the molecules lie on the surface; at negative potentials the fluorescence is high, which indicates that the DNA molecules extend from the surface.

Measurements of the kind depicted in Figure 3 have been repeated with a DNA layer in its single- and double-stranded hybridization states in electrolyte solutions containing various concentrations of monovalent salt ([NaCl] = 0.1, 1, 10, 100, 1000 mM, pH $\approx$ 4.7). For each salinity condition, the fluorescence response to the shown bias sequence was recorded at different temperatures (1, 10, 20, 30, 40, and 50 °C). We inferred the distance of the DNA's top end to the metal surface from the measured fluorescence intensity using the energy-transfer calculations described in the Materials and Methods section (cf. Figure 2). The obtained DNA layer height (distance from the DNA's distal end to the surface) is shown as a function of electrode potential, temperature, and solution salinity in Figure 4.

In solutions containing very high concentrations of salt ($C_s$ = 1000 mM, Figure 4A,B), the DNA layer conformations are exceptionally robust; that is, the molecules are insensitive to external influences. Variations in the surface potential do not alter the conformation of the ss- or ds-DNA layers, nor do temperature changes affect the layers considerably. The conformations of single- and double-stranded molecules are, however, remarkably different. While ds-DNA extends far from the surface, ss-DNA adopts a compacted (compressed) state. In its double-stranded form, the layer is twice as high as in the single-stranded form.

In an intermediate salt concentration regime ($C_s = 10-100$ mM), DNA of both hybridization states responds to externally applied potentials. For positive electrode bias the negatively charged molecules are attracted to the surface, while for negative bias the molecules are repelled from the surface. We note that the terms "positive" and "negative" are used with respect to the electrode's potential of zero charge (pzc) here. At very negative as well as very positive potentials, the DNA layer height levels off. For example, the conformation of ds-DNA at $C_s$ = 10 mM (Figure 4E) can be manipulated most efficiently when switching the potential between $-0.6$ and $-0.2$ V (vs MCH coated Pt reference); the application of more positive or more negative potentials does not lead to significant further changes in the DNA layer conformation. The ionic strength of the solution affects the DNA conformation. When the salt concentration is decreased, the effect of the applied electrode potential becomes stronger. Also, it takes "less positive" potentials to attract the DNA to the surface. The influence of temperature on the DNA conformation is remarkably different for single- and double-stranded molecules. While ds-DNA layers are fairly insensitive to temperature changes, ss-DNA becomes "activated" at elevated temperatures, and reactions to variations in the surface potential are more pronounced. For a given surface potential, in particular for negative potentials, we observe that ss-DNA stretches away from the surface when the temperature is increased. It is also interesting that ss-DNA may not be pulled to the surface as efficiently as ds-DNA molecules (cf. Figure 4E,F for low temperatures and positive potentials).

In solutions of very low salt concentrations ($C_s = 0.1-1$ mM), ds-DNA cannot be investigated because the duplex is not thermally stable. On the other hand, ss-DNA shows a most intriguing behavior, as it may be stretched out to an extreme degree. Especially at high temperatures, the single strands extend exceptionally far from the surface and reach even further into solution than the maximum extension measured for double strands.

Over a wide range of salt concentrations from $C_s$ = 100 mM down to 0.1 mM, we observe that the electric potentials at which the DNA molecules can be switched between an extended and compact conformation gradually shift to more negative values. While for $C_s$ = 100 mM the DNA conformation switches from "standing" to "lying" when sweeping the potential positively across +0 V (Figure 4D), the transition occurs at ca. $-0.5$ V for $C_s$ = 1 mM (Figure 4G).

To test the formation and stability of base-pair interactions, we performed thermal denaturation (melting) experiments in solution. In optical absorption measurements, the disintegration

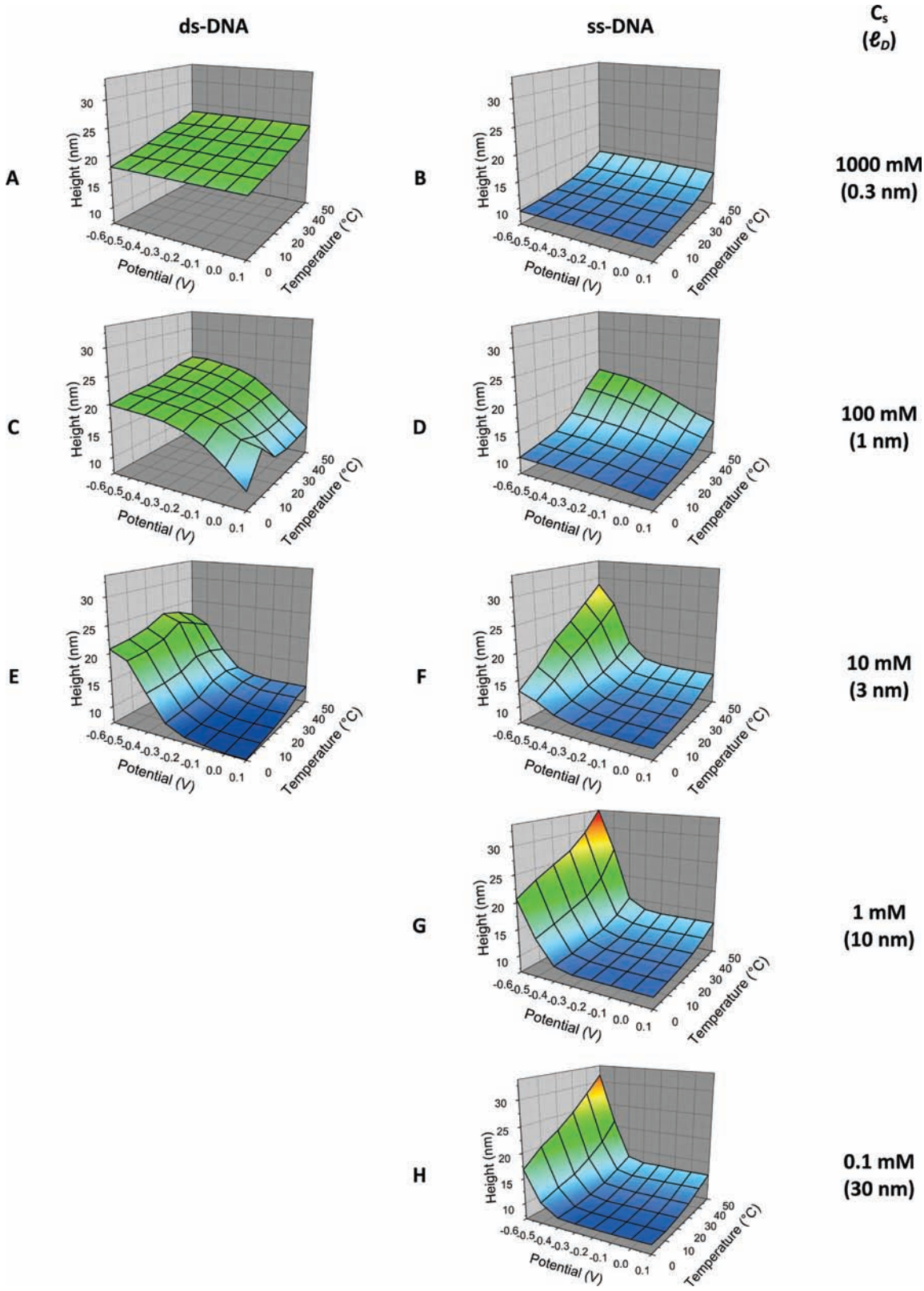


***Figure 4.*** Extension of double-stranded (left) and single-stranded (right) 72mer DNA molecules from an electrically biased gold surface. The layer height (distance from the DNA's top end to the surface) is plotted as a function of applied electrode potential (vs MCH-coated Pt quasi-reference; Pt $\approx +0.4$ V vs Ag/AgCl) and temperature. The concentration of NaCl in solution ($C_s$) is indicated on the right, along with the corresponding Debye screening length ($l_D$).

of base pairs at elevated temperatures can be evidenced by a characteristic increase in the DNA absorption at 260 nm (DNA hypochromism). Figure 5 shows melting curves of single- and double-stranded DNA in solutions of varying salt concentrations. Double-stranded samples exhibit typical DNA melting profiles with sharp double-stranded to single-stranded transitions centered at the melting temperature, $T_m$ (Figure 5A). In solutions of low ionic strength, the duplex is less stable, and thus low $T_m$

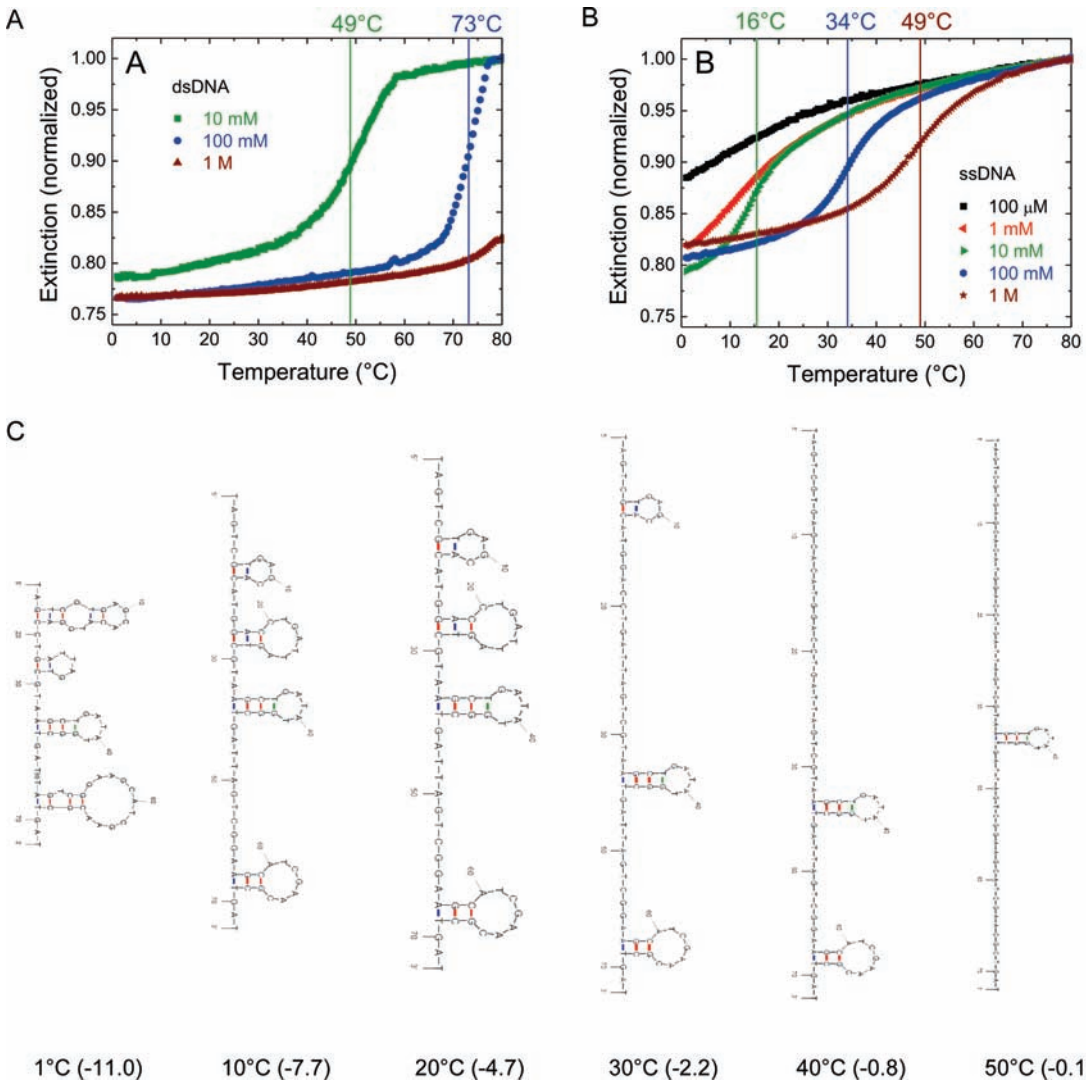


***Figure 5.*** Thermal denaturation (melting) of DNA in solution. The optical extinction at a wavelength of 260 nm is measured for (A) prehybridized double-stranded DNA and (B) single-stranded DNA in solutions of varying NaCl concentrations. Data are normalized to extinction values measured at 80 °C, i.e., to the disentangled single-stranded state (except for 1 M ds-DNA data, which were rescaled to match the 100 mM data measured at 1 °C). Panel C shows the most stable hairpin structures in 100 mM NaCl solutions as predicted by DINAMelt[18,19] calculations (see the Supporting Information, Figure S1 and Table S1). $\Delta G$ values in kcal/mol are listed in parentheses.

values are observed.[30−32] For instance, duplex melting is found to occur at $T_m$ = 73 °C in 100 mM NaCl solutions, whereas the melting temperature drops to 49 °C in solutions containing only 10 mM salt.

Figure 5B depicts the melting behavior of single strands. First and foremost, it seems remarkable that the single-stranded samples show signatures of base-pair melting at all, since a designated fully complementary sequence for duplex formation was not present. Considering the substantial length of the used 72 nucleotide (nt) sequence, however, it is not surprising that partial sequences along the 72mer are complementary and facilitate binding between (short) segments. Although the sequence was chosen with the intent to minimize the occurrence of self-complementary segments, this effect cannot be avoided totally when dealing with sequences containing a considerable number of nucleotides. In principle, inter- and intra-strand binding is possible, the latter leading to secondary (folded) structures such as hairpins. Computer simulations performed with the DINAMelt server[18,19] predict a number of thermodynamically stable secondary structures. Figure 5C depicts the structures that are most stable in 100 mM NaCl solution; for other salt concentrations, see the Supporting Information, Figure S1. The single strand features many hairpins and is strongly folded at low temperatures. At high temperatures, i.e., above ∼40 °C, most of the hairpins have melted and the ss-DNA exists in a mostly linear, extended conformation. Experimental data corroborate the simulation results: The low melting temperatures and broad phase transitions indicate the melting of comparably short double-stranded segments. The melting temperature drops below room temperature for salt concentrations lower than 10 mM, because low ionic strength destabilizes the double helix.[33,34] For [NaCl] = 100 $\mu$M, stable secondary structures do not exist; the slight extinction decrease with decreasing temperature most

(30) SantaLucia, J. *Proc. Natl. Acad. Sci. U.S.A.* **1998**, *95*, 1460–1465.
(31) Schildkraut, C.; Lifson, S. *Biopolymers* **1965**, *3*, 195–208.
(32) Tan, Z. J.; Chen, S. J. *Biophys. J.* **2006**, *90*, 1175–1190.
(33) Jost, D.; Everaers, R. *Biophys. J.* **2009**, *96*, 1056–1067.
(34) Owczarzy, R.; Moreira, B. G.; You, Y.; Behlke, M. A.; Walder, J. A. *Biochemistry* **2008**, *47*, 5336–5353.

likely originates from the stacking of bases which occurs at low temperatures.[35]

## Discussion

**High Ionic Strength—Weak Electrical Interactions.** In solutions containing very high concentrations of added salt ([NaCl] = 1 M), the abundant ions screen other charges extremely efficiently so that electrostatic potentials decay within subnanometer distances ("zero-field case"), cf. Figure 1. As a result, the electrostatic potential emanating from the surface is too short-ranged to affect the DNA considerably. Its influence is outweighed by thermal motions (cf. the dashed $k_BT$ line in Figure 1), which randomize the molecular conformations. Also, the absence of long-range electrostatic interactions influences the intrinsic structure of the DNA molecules, as electrically mediated correlations (self-repulsion) of segments along the charged DNA backbone are suppressed. This bears particular consequences for single-stranded DNA, because it lacks the inherent mechanical rigidity of the double helix. Note that, whereas double-stranded DNA features a persistence length of 50 nm, the bare persistence length (i.e., without electrostatic contributions) of single-stranded DNA is of the order of 1 nm.[36−39]

A striking difference is observed for DNA layers of different hybridization states (Figure 4A,B), which is schematically depicted in Figure 6A: ds-DNA extends from the surface widely, while ss-DNA adopts a compacted state. In fact, the ds-DNA conformation is remarkably upright: it almost matches the maximally measured height values and resembles the data obtained for ds-DNA at negative potentials in solutions of low salinity (under these conditions, the DNA is expected to stand upright on the surface, as will be discussed below).

In order to understand the reasons why the ds-DNA is "standing" on the surface, we consider a most simple model assuming that the ds-DNA behaves like an infinitely thin, end-tethered rod. Owing to thermal fluctuations, the rod's orientation with respect to the surface changes rapidly over time; however, the time resolution of our experiment does not allow us to follow these Brownian motions in real time. Instead, we observe a time-averaged height of the upper DNA end above the surface. Noting that the rod's out-of-plane rotation features two degrees of freedom along the in-plane directions $x$ and $y$, we may calculate the time-averaged angle,

$$\langle\theta\rangle = \int \mathrm{d}\theta\, \theta \cos\theta / \int \mathrm{d}\theta \cos\theta = 33° \qquad (3)$$

$\theta$ being the angle between the rod and the surface plane. Accordingly, the top rod end resides at a height above the surface corresponding to approximately half of the rod length. Comparing this estimate to the experiment, we find that it underestimates the observed DNA height.

Thus, we refine the model by considering the finite diameter of the DNA duplex as well as the fact that the DNA is asymmetrically tethered to the surface by a $C_6$-linker from one strand only. We propose that the upright conformation of the ds-DNA is caused by steric repulsions between the lowest base-pair and the MCH-SAM that backfills the gold surface between DNA molecules. MCH features the same length as the $C_6$-linker that tethers one strand to the surface. Thus, if the duplex tilts toward the surface, it must do so by turning around a pivot point at the top of the $C_6$ linker in a direction opposing the surface-proximal part of the complementary strand, which otherwise would be required to dip into and displace the MCH layer, as can be seen in the magnified inset of Figure 6A. In that context, it is important to note that the rod-like ds-DNA molecule can rotate not only around its tethered end point (out-of-surface-plane rotation) but also around its long axis. Owing to the very different degrees of friction impeding these two motions, revolutions around the long molecular axes occur on a substantially shorter time scale than out-of-surface-plane rotations around the DNA's end point.[40] Hence, averaged over time, the surface-proximal part of the complementary strand points toward all in-plane directions with the same probability, and thus a preferential direction for the DNA duplex to tilt toward the surface does not exist. As a result of these steric interactions between the surface-proximal part of the complementary strand and the MCH layer, the DNA adopts an upright orientation.

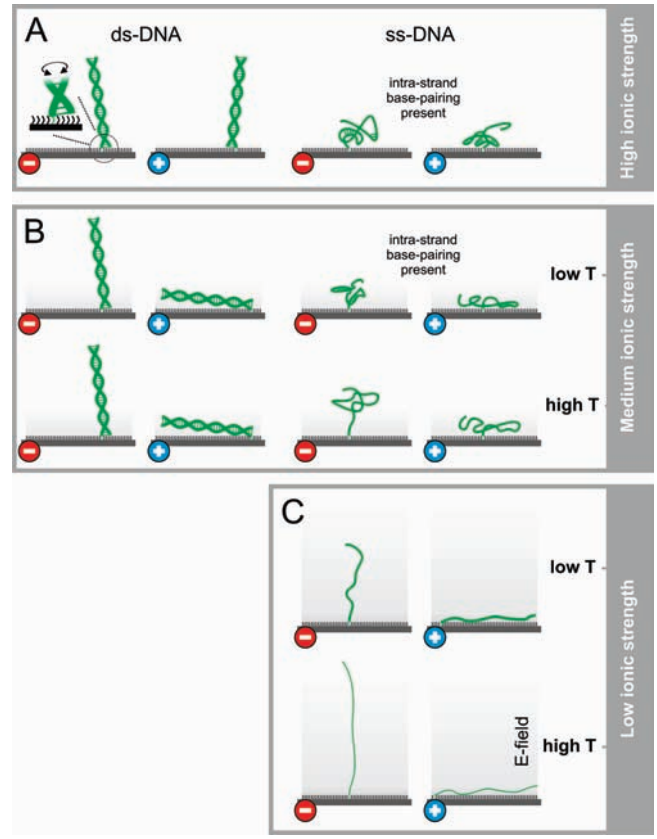


***Figure 6.*** Schematic representation of the DNA conformation on negatively and positively charged surfaces in electrolyte of varying ionic strength.

The ss-DNA layer features a compact conformation and reaches merely half of the ds-DNA layer height. Its compact state is a consequence of the tendency of flexible polymers to form coils and, in particular, the occurrence of secondary structures, i.e., hairpins (loops which are stabilized by the base-pairing of different segments along the sequence). Melting

(35) Yakovchuk, P.; Protozanova, E.; Frank-Kamenetskii, M. D. *Nucleic Acids Res.* **2006**, *34*, 564–574.
(36) Lu, Y. J.; Weers, B.; Stellwagen, N. C. *Biopolymers* **2001**, *61*, 261–275.
(37) Porschke, D. *Biophys. Chem.* **1991**, *40*, 169–179.
(38) Smith, S. B.; Finzi, L.; Bustamante, C. *Science* **1992**, *258*, 1122–1126.
(39) Tinland, B.; Pluen, A.; Sturm, J.; Weill, G. *Macromolecules* **1997**, *30*, 5763–5765.
(40) Tirado, M. M.; Martinez, C. L.; Delatorre, J. G. *J. Chem. Phys.* **1984**, *81*, 2047–2052.

curves measured in 1 M NaCl solution show the occurrence of a stable secondary structure with $T_m = 49$ °C. Simulations[18,19] predict a hairpin structure with the same melting point, which is depicted in Figure S1 and Table S1 in the Supporting Information.

**Medium Ionic Strength—Moderate Electrical Interactions.** In solutions containing moderate to low concentrations of ions ($C_s = 10-100$ mM), electric interactions have a significant influence on the DNA's conformation. The interaction range scales with the Debye screening length, which is 1 and 3 nm for $C_s = 100$ and 10 mM, respectively. If we consider a DNA duplex that stands upright on the surface, 3 bp (for $C_s = 100$ mM) or 9 bp (for $C_s = 10$ mM) are located within a region of strong electric fields above the surface.

For the rigid ds-DNA, the interaction of the surface field with a few base pairs is strong enough to align the molecules against the randomizing effect of Brownian motions. Plateaus of maximal and minimal layer height are reached when applying negative or positive electrode potentials of merely a couple hundred millivolts. Saturation at a maximal height value for negative potentials indicates that the molecules are standing almost fully upright on the surface. At low temperatures and positive potentials, the DNA duplexes lie almost flat on the surface; the data shown in Figure 4 suggests tilt angles below 20°.

ss-DNA molecules cannot be manipulated as efficiently as ds-DNA molecules by electric fields. This is a consequence of the flexibility of the single strands in conjunction with the short-range electric field that emanates from the electrode surface. Panel B in Figure 6 schematically depicts how only the surface-proximal part of the charged DNA backbone, which resides in the strong field region ($z \leq l_D$), is aligned by repulsive electric forces. The upper DNA part is not exposed to strong electric fields, and thus its conformation is randomized by thermal motions. At high ionic strength ($C_s \geq 100$ mM) and low temperatures, ss-DNA hardly reacts to changes in the electrode potential. At elevated temperatures, the height of single-stranded layers increases and the response to electric fields is more pronounced. This effect can be explained by the melting of DNA hairpins, which keep the ss-DNA folded at low temperatures. At higher temperatures the hairpins unfold, the effective length of the DNA polymer is enhanced, and the molecules extend farther from the surface. This interpretation is supported by the agreement of the observed layer height increase with the measured $T_m$: In the case of the $C_s = 100$ mM data, the height increase in the temperature range from 30 to 50 °C agrees well with the melting curve measured in bulk solution ($T_m = 34$ °C, Figure 5B). Data for $C_s = 10$ mM show a similar trend which commences at lower temperatures, corresponding to the lower melting temperature of the secondary structures ($T_m = 16$ °C, Figure 5B) at lower ionic strength. Yet, remarkably, this trend continues above 30 °C, where bulk solution measurements show that the hairpin has fully melted. This will be discussed in more detail below.

In general, the lowest height values for attractive electrode potentials (+0.1 V) are observed at low temperatures, but ds-DNA may be pulled to the surface more efficiently than ss-DNA. This can be understood by evoking entropy, which counteracts the electrically induced order of the system and results in repulsion (reflection) of the molecules from the hard wall. As ss-DNA features greater flexibility and hence more degrees of freedom than ds-DNA, entropic effects are more pronounced; i.e., the entropic penalty to force a ss-DNA molecule to adopt a state of high order by lying flat on the surface is greater than for an essentially linear ds-DNA molecule. These observations are in accordance with hydrodynamic simulations.[41,42]

**Low Ionic Strength—Strong Electrical Interactions.** In solutions of low ionic strength, screening effects are comparably weak, and thus charges interact over long distances. The self-repulsion of negatively charged sites along the DNA backbone is significant, which prevents the formation of secondary structures. Double-stranded DNA is not stable under these conditions; neither are folded hairpin structures of single strands at $C_s = 0.1$ mM (cf. melting experiments presented in Figure 5). Below 20 °C, minor stacking interactions probably occur for $C_s = 0.1$ mM, while for $C_s = 1$ mM the onset of intra-strand interactions is more pronounced.

The extreme extension of ss-DNA observed for repulsive negative electrode potentials and high temperatures is very remarkable, as the end-to-end distance of the ss-DNA molecules (>30 nm) even exceeds the molecular contour length of their double-stranded counterparts (24 nm).

To put this finding into perspective, it is instructive to compare it to a basic model for flexible polymers. According to the freely jointed chain (FJC) model, the mean end-to-end distance of DNA in a coiled state is given by

$$\sqrt{\vec{R}^2} = \sqrt{Nl^2}$$

where $N$ is the number of segments (i.e., nucleotides, $N = 72$) and $l$ is the internucleotide spacing. Even when inserting the maximally achievable value ("stretched" bonds) for the internucleotide spacing, $l = 0.7$ nm, the FJC model predicts an end-to-end distance of merely 6 nm, which clearly underestimates the experimental observation. The failure of the model suggests that the single-stranded 72 nt DNA is in fact not flexible but adopts a rather stiff and straight conformation. Following this notion and assuming that the single strands stand upright on the surface, we may estimate an apparent internucleotide spacing of $l_{ss} \approx 0.45$ nm, which denotes a stretching by 30% compared to the double helix ($l_{ds} \approx 0.34$ nm).

In the following we discuss reasons for the extreme extension of the ss-DNA layer and propose that four factors play an essential role: (i) the long-range surface field, (ii) electrostatic stiffening of the DNA, (iii) temperature-induced DNA stretching by counterion release, and (iv) disruption of base stacking.

(i) Due to the weak screening in electrolytes of low ionic strength,the electric potential and field which emanate from the negatively biased surface are very long ranged (see Figure 1). Note that the screening lengths for $C_s = 1$ mM and $C_s = 0.1$ mM are $l_D = 10$ nm and $l_D = 30$ nm, respectively, which is comparable to the molecular contour lengths of the oligonucleotides used, $L_{ds}^{72} = 24$ nm and $L_{ss}^{72} < 50$ nm (again assuming a fully extended backbone with an internucleotide spacing of $l_{ss} \approx 0.7$ nm). Thus, in contrast to the previously discussed conditions of higher ionic strengths, the surface field interacts with many (all) charged groups along the DNA backbone, which results in an efficient repulsion from the surface.

(ii) The mechanical rigidity of ss-DNA is known to depend on the ionic strength of the environment. According to the theory of Odijk[43] and Skolnick and Fixman[44] (OSF), the persistence length $l_p$ of a charged polymer can be written as

(41) Sendner, C.; Kim, Y. W.; Rant, U.; Arinaga, K.; Tornow, M.; Netz, R. R. *Phys. Status Solidi A—Appl. Mater. Sci.* **2006**, *203*, 3476–3491.
(42) Rant, U.; Arinaga, K.; Tornow, M.; Kim, Y. W.; Netz, R. R.; Fujita, S.; Yokoyama, N.; Abstreiter, G. *Biophys. J.* **2006**, *90*, 3666–3671.

$$l_p = l_0 + l_e \quad (4)$$

where $l_0$ and $l_e$ are the bare and electrostatic contributions to the polymer's total persistence length, respectively. The bare persistence length of ss-DNA is merely 2−3 nm.[39] The electrostatic persistence length is given by

$$l_e = \frac{l_B}{4}\lambda^2 {l_D}^2 \quad (5)$$

with the Bjerum length

$$l_B = e^2/4\pi\varepsilon\varepsilon_0 k_B T \quad (6)$$

($l_B$ corresponds to the distance at which the strength of Coulomb interactions equals $k_BT$; $l_B$ = 0.7 nm in water at room temperature) and the line charge density $\lambda$.

$l_e$ becomes important for concentrations of monovalent salt of the order of 10 mM ($l_e \approx 10$ nm) and quickly exceeds the lengths of typical oligonucleotides for lower ionic strength ($l_e \approx 100$ nm for $C_s = 1$ mM, $l_e \approx 1000$ nm for $C_s = 0.1$ mM). Under the latter conditions, single-stranded oligonucleotides with fewer than 100 nt are expected to be fairly inflexible and rod-like. In fact, the stiffening of ss-DNA in solutions of low ionic strength has been observed experimentally also by other authors, e.g., by Tinland et al.[39] or Murphy et al.[45]

These considerations suggest that in solutions of low ionic strength, ss-DNA behaves similar to ds-DNA at higher ionic strength: the single strands become rod-like and stand almost upright on the surface under the influence of negative electrode potentials.

(iii) The temperature-induced stretching of ss-DNA at negative electrode potentials is particularly intriguing. Note how the layer height measured at −0.6 V increases almost by a factor of 2 (from 17 to 31 nm) when the temperature is elevated from 1 to 50 °C. At first glance, this cannot be understood in terms of a mechanical stiffening of the single strands within the OSF theory, because the electrostatic persistence length does not seem to be temperature dependent: $l_e \propto l_B {l_D}^2 \propto T^{-1}T \neq f(T)$. In this scaling argument, however, the line charge density $\lambda$ was assumed to be constant, which does not hold when taking counterion condensation phenomena into account. In the following we will discuss the temperature dependence of $\lambda$ in the context of counterion condensation and reveal the consequences on DNA stiffness.

According to counterion condensation theory,[17] the behavior of linear polyelectrolytes is characterized by the charging parameter $\xi$, which is defined as the ratio of the Bjerum length $l_B$ and the distance $b$ between two consecutive charges along the polymer:

$$\xi = \frac{l_B}{b} \quad (7)$$

For highly charged linear polyelectrolytes ($\xi > 1$) like DNA, electric repulsions from like charges along the polymer bring about an enormous electrostatic self-energy. This unfavorable condition is relaxed by counterions which condense onto the polymer from solution and screen the intrinsic charges along the polyelectrolyte. As this localization of ions from solution occurs at entropic cost, an equilibrium state adjusts at which the decrease in electrostatic self-repulsion and decrease in entropy are balanced.

***Table 1.*** Temperature Dependence of the Bjerum Length ($l_B$), the Debye Screening Length ($l_D$), the Charging Parameter ($\xi$) of ss-DNA, the Corresponding Effective Charge ($q_{eff}$), and the Electrostatic Persistence Length ($l_e$) in Electrolyte Solution Containing 1 mM Monovalent Salt

| $T$ (°C) | $l_B$ (Å) | $l_D$ (nm) | $\xi^a$ | $q_{eff}$ (e) | $l_e$ (nm) |
|---|---|---|---|---|---|
| 1 | 7.6 | 9.3 | 1.90 | 0.53 | 28 |
| 25 | 7.0 | 9.7 | 1.75 | 0.57 | 34 |
| 50 | 6.5 | 10.1 | 1.62 | 0.62 | 40 |

[a] From eq 7 with $b = 0.4$ nm.

In this state, the effective value of a charged site along the polymer becomes (for monovalent counterions)

$$q_{eff} = \frac{e}{\xi} = \frac{eb}{l_B} \propto bT \quad (8)$$

The temperature dependence of $q_{eff}$ translates to the effective line charge density, so that

$$\lambda_{eff} = \frac{q_{eff}}{b} \propto T \quad (9)$$

After inserting eqs 9, 6, and 2 into the expression for the electrostatic persistence length (eq 5), we obtain

$$l_e \propto l_B {\lambda_{eff}}^2 {l_D}^2 \propto T^2 \quad (10)$$

and find that $l_e$ scales with $T^2$.

In solutions of low ionic strength, this temperature dependence has profound consequences on the DNA stiffness, as can be seen from Table 1, which lists several screening parameters along with $l_e$ for several examples. When the temperature is increased from 1 to 50 °C, $l_e$ increases from 28 to 40 nm, which denotes a relative increase of 40%.

It is important to note that the values listed in Table 1 were calculated assuming a constant distance $b$ between consecutive charges along the polymer. Because every nucleotide features one negative charge, $b$ corresponds to the internucleotide spacing along the phosphate backbone for ss-DNA. However, it is difficult to estimate the internucleotide spacing in ss-DNA, since the backbone is very flexible. In addition, the tendency of bases to stack on top of each other depends on the type of base and neighboring bases, so that the local internucleotide spacing may be modulated by the nucleotide sequence. We can estimate an upper limit of the internucleotide spacing by adding up the bond lengths of a fully extended backbone, which amounts to 0.7 nm.

The reasoning above leads to the following interpretation: when the temperature is increased, the entropic penalty of keeping counterions localized at the DNA backbone grows. Consequently, counterions are released into solution, and the effective charge of the DNA backbone increases. This results in an enhanced self-repulsion of the like-charged, deprotonized sites along the backbone and leads to a stretching and stiffening of the DNA molecule.

An alternative explanation for the thermally induced stretching is that base-stacking interactions are disrupted at elevated temperatures, which has been shown, for instance, by Zhou et al.,[46] Ramprakash et al.,[47] and Yakovchuk et al.[35] The latter investigated also the influence of salinity on stacking and found

(43) Odijk, T. *J. Polym. Sci., Part B: Polym. Phys.* **1977**, *15*, 477–483.
(44) Skolnick, J.; Fixman, M. *Macromolecules* **1977**, *10*, 944–948.
(45) Murphy, M. C.; Rasnik, I.; Cheng, W.; Lohman, T. M.; Ha, T. J. *Biophys. J.* **2004**, *86*, 2530–2537.

that low salinity weakens the stacking stability. In neutron scattering experiments, Zhou et al.[46] observed a significant stretching of a 10 nt single-stranded DNA when the temperature was increased over the base-stacking melting point. Indications for the occurrence of base stacking at low temperatures, even at very low ionic strength (0.1 mM), are also present in this work in the melting curves of Figure 5B. It is very likely that the unstacking of bases contributes to the stretching observed in Figure 4G,H; as a consequence of the low salinity and the resulting electrostatic stiffening, the unstacked single strands probably feature a significant rigidity, which explains why their orientation on the surface can be manipulated efficiently by electric fields.

Finally, we note for completeness that electrostatic stiffening effects are not important for double-stranded DNA, which features a considerable intrinsic persistence length ($l_0 \approx 50$ nm) due to the structural rigidity of the double helix. The electrostatic contribution to the persistence length would become significant ($l_e \geq l_0$) only in solutions of very low salinity ($C_s \ll 10$ mM), but the double helix is thermally unstable under these conditions, so that double strands promptly dissociate into single strands.

**Potential of Conformation Transition.** So far we have seen that positive electrode potentials induce a compact DNA conformation while negative potentials induce an extended DNA conformation; however, the terms "negative" and "positive" have been used loosely up to now without defining a point of reference. Here we address this fundamental issue and denote the potential value at which the DNA conformation flips from an extended to a compact state (or vice versa) as the *potential of conformation transition (pct)*.

The experimental results show that the pct is largely temperature independent, but also that it clearly varies with the solution salinity. We observe a gradual shift of the pct from positive to negative values upon decreasing the NaCl concentration: pct(100 mM) $\approx$ 0.0 V, while pct(0.1 mM) $\approx -0.5$ V. Other authors, who have also observed conformational changes of DNA layers, report diverse potential values for which the conformation transition occurs, ranging from +0.5 V (vs Ag wire, in 50 mM NaCl, 100 mM $MgCl_2$)[1] and ca. +0.4 V (vs SCE, in 10 mM Tris, 10 mM NaCl)[6] to ca. 0.0 V (vs SCE, in 10 mM phosphate buffer).[5,48] In that respect, it is important to note that the grafting density of the DNA layers plays a significant role: we have observed that high-density layers require more positive potentials to be attracted to the surface, which most likely results from crowding that impedes the molecules sterically. Also, we observed that this effect is more pronounced for ds-DNA layers than for ss-DNA layers, which supports the crowding argument. We believe that the discrepancies in the pct reported from various groups arise partly from the different compositions of the electrolytes used and partly from different layer preparation conditions, which result in varying grafting densities. In particular, for scanning probe studies high grafting density layers have been investigated, whereas in this study we have been taking special care (electrical desorption steps) to prepare ultra-low-density DNA layers for which steric interactions can be excluded.

In order to switch the electrical interaction between the DNA and the substrate from repulsive to attractive (or vice versa), the charge on the electrode surface must be reversed. In electrochemical terms, the polarity of a surface changes when the applied potential is swept across the electrode's *potential of zero charge (pzc)*. The pzc depends on surface properties like the crystal orientation of the exposed facets, electrolyte composition, surface adsorbates, etc. and, in general, is not necessarily 0 V.

Intuitively one might assume that the pct coincides with the pzc. In fact, the pzc of hydroxyl-terminated alkanethiol-coated gold electrodes has been reported to be $-0.1$ V (vs SCE, i.e., $-0.3$ V for the Pt reference used here),[49] which agrees well with our observations of the pct at intermediate salt concentrations (10−100 mM). It should be noted, however, that comparisons of pzc values are generally problematic because often pzc data for the conditions of interest do not exist due to experimental limitations. In particular for Au electrodes, meaningful pzc values in NaCl-containing buffers have not been reported.

The observed negative shift of the pct with decreasing electrolyte ionic strength is particularly intriguing. It is straightforward to assume that the pct shift results from a shifting pzc. For bare Au surfaces, it is known that the pzc of Au (111) surfaces shifts positively with decreasing concentration of chloride salts because $Cl^-$ ions adsorb onto the Au at high concentrations.[50] Since attempts to measure the pzc as a function of solution salinity by the capacitance method[51] were not successful, we measured the equilibrated *open circuit potential* (*ocp*) instead, because changes in the pzc are expected to affect the easily observable ocp as well.

We found that the ocp was ca. $-0.25$ V (vs Pt) at 100−1000 mM NaCl and that it shifted slightly positive to $-0.1$ V (vs Pt) when the NaCl concentration was decreased to 0.1−1 mM, indicating the expected adsorption of $Cl^-$ ions on Au at high NaCl concentrations.[50] However, this trend contradicts the observed negative pct shift, which means that the pct shift is not caused by a corresponding shift of the pzc.

We propose that image charge effects cause the negative shift of the pct with decreasing ionic strength. It is known that a charge close to a metal polarizes the metal; i.e., it creates an image charge of opposite sign within the metal. In this way, an attractive force arises between the free charge and the metal, which (in the absence of other forces) will cause the free charge to adsorb onto the metal surface. In electrolytes, the interaction between the charge and its image is screened by ions in solution and thus is effectively weakened. The resulting interaction potential, $U$, as a function of the distance, $z$, between the charge and the metal may be written in the Debye−Hückel limit[52,53] as

$$\frac{U(z)}{k_B T} \approx \frac{l_B}{4z}\left(\frac{\varepsilon - \varepsilon_1}{\varepsilon + \varepsilon_1}\right)\exp(-2z/l_D) \qquad (11)$$

In eq 11, the Debye length $l_D$ again appears as a characteristic length which scales the exponential decay of the interaction

(46) Zhou, J.; Gregurick, S. K.; Krueger, S.; Schwarz, F. P. *Biophys. J.* **2006**, *90*, 544–551.
(47) Ramprakash, J.; Lang, B.; Schwarz, F. P. *Biopolymers* **2008**, *89*, 969–979.
(48) Wackerbarth, H.; Grubb, M.; Zhang, J. D.; Hansen, A. G.; Ulstrup, J. *Angew. Chem., Int. Ed.* **2004**, *43*, 198–203.
(49) Becka, A. M.; Miller, C. J. *J. Phys. Chem.* **1993**, *97*, 6233–6239.
(50) Li, N. H.; Lipkowski, J. *J. Electroanal. Chem.* **2000**, *491*, 95–102.
(51) Bard, A. J.; Faulkner, L. R. *Electrochemical Methods: Fundamentals and Applications*, 2nd ed.; Wiley: New York, 2001.
(52) Dobrynin, A. V.; Rubinstein, M. *Prog. Polym. Sci.* **2005**, *30*, 1049–1118.
(53) Netz, R. R. *Phys. Rev. E* **1999**, *60*, 3174–3182.

potential. $\varepsilon$ and $\varepsilon_1$ are the dielectric constants of the electrolyte and the metal, respectively. Since $\varepsilon_1$ is strongly negative, the potential becomes negative, and hence the interaction is attractive. In view of eq 11, we can rationalize the observed ionic strength dependence of the pct: Due the attractive image charge interaction, the charged DNA generally tends to adsorb onto the surface. The external application of negative bias potentials repels the DNA from the surface, but the DNA will detach from the surface only when the influence of the repulsive external bias exceeds the image charge attraction. Since the image charge attraction scales with the ionic strength, i.e., the attraction becomes stronger with decreasing solution salinity, more negative (stronger) external potentials are required to effectively repel the DNA from the surface, and hence the pct becomes increasingly negative at low ionic strength.

## Conclusion

In solutions of high ionic strength, where electric interactions are almost completely suppressed due to the presence of high concentrations of ions in solution (zero-field case), ds-DNA and ss-DNA adopt very different conformations on the surface. While single strands take on a compact state, double strands stand on the surface, most likely due to steric interactions of the surface-near part of the rigid helix with the underlying alkanethiol layer. The molecular conformations are extremely "robust" in that neither variations in the surface potential nor temperature changes substantially affect the molecules.

In an intermediate salinity range, electric fields emanating from the charged surface interact with the surface-proximal parts of the DNA oligonucleotides. It is possible to efficiently manipulate the DNA conformation by the application of bias potentials to the supporting metal electrodes. The effectiveness of the induced conformation change is higher for double- than for single-stranded oligonucleotides because the former behave like rigid rods. Whereas the conformation change of the duplex may be viewed as a tilting motion about the chemical tether (pivot point), the structural change of the single strands may rather be regarded as a folding/unfolding process onto/from the surface.

At low ionic strength, the structural properties of ss-DNA change dramatically. Due to electrostatic repulsions between charged sites along the DNA backbone, the electrostatic contribution to the persistence length strongly increases; consequently, the single strands stiffen and become rod-like. In this state the extension of ss-DNA from the surface may be manipulated very efficiently by electric fields.

The conformation temperature dependence of single- and double-stranded DNA molecules is very different, except at high salt concentrations, for which both ss-DNA and ds-DNA are fairly insensitive to temperature changes. While ds-DNA layers generally retain this robustness against temperature changes up to the duplex melting temperature, ss-DNA layers exhibit profound conformation changes upon temperature variations. In an intermediate salinity range, the conformation changes can be attributed mainly to the melting of intra-strand base pairs, i.e., the melting of short duplexes that keep the otherwise single-stranded molecules partly folded. A very intriguing behavior was revealed in low-salinity solutions: ss-DNA stretches out substantially with increasing temperatures. This phenomenon is possibly caused by the entropy-driven release of counterions from ss-DNA, the disruption of base stacking at elevated temperature, or a combination of both. As a consequence, the effective charge density along the DNA polymer increases and leads to an enhanced electrostatic stiffening/stretching of the otherwise flexible single strands.

Analysis of the *potential of conformation transition* show that, in solutions of decreasing ionic strength, increasingly negative electrode potentials must be applied in order to effectively repel the DNA from the surface. This behavior could be attributed to the screened image charge attraction which must be overcome by the externally applied negative bias.

In conclusion, the obtained results may serve as general design guidelines for the construction and operation of functional interfaces such as actively controlled DNA surfaces for the detection of DNA or protein targets.

**Acknowledgment.** We are very thankful to Gerhard Abstreiter for his support and to Roland Netz for helpful discussions. Financial support is gratefully acknowledged from the TUM Institute for Advanced Study (IAS), the TUM International Graduate School of Science and Engineering (IGSSE), the Fujitsu Laboratories, and the Nanosystems Initiative Munich (NIM).

**Supporting Information Available:** Calculated secondary structures and thermodynamic properties of 72 nt DNA; calculated apparent quantum yield and fit function for Cy3 above a gold surface; influences of temperature, solution salinity, and DNA hybridization state on Cy3 fluorescence; bright-field and epi-fluorescent images of bare Au and DNA-Cy3-modified Au electrodes. This material is available free of charge via the Internet at http://pubs.acs.org.

JA908727D